The Marine Natural Product Adociasulfate-2 as a Tool To Identify the MT-Binding Region of Kinesins†

Sébastien Brier,*,‡,§,|| Eugénie Carletti,§,⊥,# Salvatore DeBonis,⊥ Elisabeth Hewat,▽ David Lemaire,‡,○ and Frank Kozielski*,⊥

Laboratoire de Spectrométrie de Masse des Protéines (LSMP), Laboratoire des Moteurs Moléculaires (LMM), and Laboratoire de Microscopie Electronique Structurale (LMES), Institut de Biologie Structurale (CEA-CNRS-UJF), 41, rue Jules Horowitz, 38027 Grenoble Cedex 1, France

Received July 11, 2006; Revised Manuscript Received September 30, 2006

ABSTRACT: Kinesins are molecular motors that transport cargo along microtubules (MTs). To move forward the motor must attach to the MT in a defined orientation and detach from it in a process that is driven by ATP hydrolysis. The knowledge of the motor−MT interface is essential for a detailed understanding of how kinesins move along MTs and how they are related to other molecular motors such as myosins or dyneins. We have used the marine natural product adociasulfate-2 (AS-2), previously identified as a MT-competitive inhibitor of conventional kinesin, to infer the secondary structure elements forming the MT interface of two human mitotic kinesins, namely, CENP-E and Eg5. AS-2 inhibits both basal and MT-stimulated ATPase activities of CENP-E (IC_{50} of 8.6 and 1.3 μM, respectively) and Eg5 (IC_{50} of 3.5 and 5.3 μM, respectively) and is a MT-competitive inhibitor of CENP-E with a K_i of 0.35 μM. Binding of AS-2 to CENP-E also stimulates the ADP release from the nucleotide-binding pocket. AS-2 is a nonspecific kinesin inhibitor targeting several superfamily members including KHC, MPP1, MKLP1, RabK6, KIFC1, KIFC3, CENP-E, and Eg5. By measuring hydrogen/deuterium exchange with mass spectrometry we have shown that the formation of the CENP-E/AS-2 complex decreases the solvent accessibility of three neighboring peptides on the same face of CENP-E. We deduce that this is the site of MT attachment and conclude that loop L11, helix α4, loop L12, helix α5, loop L8, and strand β5 constitute the main MT interface of the CENP-E motor domain. Similarly for Eg5/AS-2, a region of increased solvent accessibility locates the MT interface of Eg5.

Molecular motors of the kinesin superfamily play important roles in intracellular transport and at several stages of the cell cycle (*1*). They bind to and move along microtubules (MTs[1]) driven by ATP hydrolysis. The function of these proteins is therefore directly related to their capacity to interact with MTs. A full understanding of the mechanism of kinesin movement requires the identification of the motor domain regions involved in MT binding. One technique used to probe protein−protein interfaces is hydrogen−deuterium exchange and mass spectrometry (H/D−MS). The rate at which peptide amide hydrogens undergo isotopic exchange is highly dependent on their environment, their solvent accessibility, and their participation in intramolecular hydrogen bonding (*2*−*4*). Consequently, the formation of protein complexes can influence the rate of exchange by excluding solvent from the binding interface. Conformational changes may also occur upon complex formation leading to a modification of the exchange rate not only at the binding interface but also at locations distal to the binding interface (*5*).

H/D exchange followed by MS has been widely used to investigate protein−protein interfaces (*6*, *7*), as well as the interaction sites of small molecules on proteins (*8*−*10*). The sensitivity of the method has been improved through the analysis of short peptide fragments that are generated after proteolytic digestion of the deuterated protein (*11*, *12*).

† This work has been funded by ARC (Association pour la Recherche sur le Cancer, Contract 5197) and the Rhône-Alpes region (Contracts 03 013690 02; 03 013690 01). S.B. was supported by a Ph.D. grant from the CNRS (Centre National de la Recherche Scientifique).

* Corresponding authors. S.B.: e-mail, s.brier@neu.edu; tel, 617-373-7279; fax, 617-373-2855. F.K.: e-mail, frank.kozielski@ibs.fr; tel, 0033-4-3878-4024; fax, 0033-4-3878-5494.

‡ LSMP.

§ Both authors contributed equally to this work.

|| Current address: The Barnett Institute, 341 Mugar Life Science Building, Northeastern University, 360 Huntington Avenue, Boston, MA 02115-5000.

⊥ LMM.

Current address: Departement de Toxicologie, Laboratoire d'Enzymologie, CRSSA, 24, avenue des Maquis du Grésivaudan, 38700 La Tronche, France.

▽ LMES.

○ Current address: Laboratoire des Interactions Protéine Métal (LIPM)−DEVM Bât 185, CEA Cadarache, 13108 Saint Paul-lez-Durance Cedex, France.

[1] Abbreviations: ACES, *N*-(2-acetamido)-2-aminoethane sulfonic acid; AS-2, adociasulfate-2; ATP, adenosine 5′-triphosphate; DMSO, dimethyl sulfoxide; EDTA, ethylenediaminetetraacetic acid; EGTA, ethyleneglycol-bis(β-aminoethyl ether) *N*,*N*,*N*′,*N*′-tetraacetic acid; H/D, hydrogen/deuterium; HPLC, high pressure liquid chromatography; IPTG, isopropyl β-D-thiogalactopyranoside; ESI, electrospray ionization; LC−MS, liquid chromatography−mass spectrometry; MS, mass spectrometry; MS−MS, mass spectrometry−mass spectrometry; *m*/*z*, mass to charge ratio; MTs, microtubules; PIPES, piperazine-*N*,*N*′-bis(2-ethanesulfonic acid); SDS−PAGE, sodium dodecyl sulfate−polyacrylamide gel electrophoresis; TFA, trifluoroacetic acid.

10.1021/bi061395n CCC: $33.50
Published on Web 12/01/2006

However with an increase in the size of the protein complex the MS analysis becomes more complex due to the large number of peptide fragments that are generated after proteolytic digestion. In order to minimize isotopic back exchange, the HPLC system must be maintained at 0 °C and the gradient optimized for speed. The "poor" chromatographic separation in some cases leads to overlapping mass peaks for coeluting peptides and hinders successful data interpretation. As a result, it is sometimes necessary to separate the different binding partners of deuterated complexes prior to protease digestion and LC−MS analysis. For example to identify directly the MT-binding region of kinesins by H/D−MS, MTs would have to be removed just after the deuteration step to avoid the generation of a large number of peptides from the αβ-tubulin heterodimer after proteolytic digestion. To obviate the need for a separation step and to reduce the complexity of the system, we used the bioactive marine natural compound adociasulfate-2 (AS-2), isolated from the marine sponge *Haliclona* sp. (also known as *Adocia* sp.) (Figure 1A) (*13*). AS-2 was shown to inhibit the MT-stimulated ATPase activity of *Drosophila melanogaster* conventional kinesin by directly competing with MT binding and appears therefore as an excellent molecular probe to infer the MT interface of several kinesins.

In this study we investigated the AS-2 binding regions of two human kinesins, CENP-E (centromere-associated protein E), a member of the kinesin-7 family, and Eg5, a member of the kinesin-5 family, and deduced the MT-binding region. Both proteins play critical roles during mitosis. Eg5 is responsible for the formation and the maintenance of the bipolar mitotic spindle. This molecular motor provides the plus-end directed force required to slide interpolar MTs during centrosome separation (*14*). CENP-E appears to be essential for monopolar chromosomes to establish bipolar attachment. This protein is thought to enhance the efficiency by which kinetochores establish stable MT contacts (*15*). Here we show that AS-2 is a MT-competitive inhibitor of the human CENP-E motor domain. Loop 11, helix α4, loop L12, helix α5, loop L8, and strand β5 appear to be the main MT-binding elements of CENP-E. In addition we found that AS-2 also modified the deuterium uptake of similar regions within the Eg5 motor domain (β4-L7-β5-L8-β5a and α4-L12-α5). Formation of the Eg5/AS-2 complex leads to a significant increase of solvent accessibility in the C-terminal part of helix α4 indicating a strong structural modification upon inhibitor binding. Most of these regions have been identified in other kinesins such as conventional kinesin, ncd, and KIF1A (L8, L11, and α4-L12-α5) (*16*−*18*), suggesting that kinesins investigated so far share a common MT interface.

EXPERIMENTAL PROCEDURES

Materials. HisTrap chromatographic columns were purchased from Amersham Pharmacia Biotech. Competent XL-10 and BL21(DE3)pLysS cells were obtained from NOVAGEN. TFA, PIPES, D_2O, DMSO, paclitaxel, lysozyme, pepsin, DNase I, and kanamycin were from Sigma-Aldrich. IPTG was purchased from ICN. Acetonitrile (CH_3CN) was bought from SDS. Chemicals for ATPase activity assays were from sources indicated by Hackney and Jiang (*19*). Ninety-six-well half-area plates were bought from Costar.

Preparation of AS-2 Solutions. AS-2 was kindly provided by Dr. Lawrence S.B. Goldstein, Howard Hughes Medicinal Institute, University of California, San Diego, La Jolla, and Dr. Timothy M. Dore, University of Georgia, Athens, Georgia 30602-2556. Lyophilized AS-2 (0.9 mg) was dissolved in 100% DMSO to a final concentration of 10 mM. Ten-fold and 100-fold dilutions in DMSO were prepared from the stock solution and stored at −20 °C. AS-2 solutions stored at room temperature tended to lose their inhibitory activity and were kept on ice during the experiments.

Overexpression and Purification of CENP-E and Eg5 Constructs. Motor domains of CENP-E_{2-341} (residues 2 to 341) and $Eg5_{2-386}$ (residues 2 to 386) were expressed and purified as described previously (*20*, *21*). Proteins were analyzed by SDS−PAGE, N-terminal sequencing, and mass spectrometry.

Purification of Bovine Tubulin and MT Polymerization. Tubulin was purified from the brain of calves younger than 24 months as described by Asnes and Wilson (*22*). Purified tubulin was aliquoted at 12 mg/mL, flash frozen in liquid nitrogen, and stored at −80 °C. Tubulin polymerization into MTs was carried out as described previously (*23*).

Mant-ADP Release Studies in the Presence of AS-2. Formation of the CENP-E/mant-ADP complex was initiated by mixing 0.19 μM CENP-E with 0.01 M mant-ADP in a final volume of 2 mL of buffer A25 (25 mM ACES/KOH at pH 6.9, 2 mM magnesium acetate, 2 mM potassium EGTA, 0.1 mM potassium EDTA, 1 mM β-mercaptoethanol, 300 mM NaCl). Mant-emission spectra were obtained by exciting samples at 285 nm and collecting the emitted fluorescence from 395 nm. The fluorimeter used was the MOS-450 from Bio-Logic Co, equipped with a 150 W Xe lamp and a double excitation monochromator. The cuvette holder used allowed the injection of reagents in microliter quantities under continuous stirring and without opening the holder thus preventing exposure to light during injection. Data acquisition and treatment was made using the Bio-Kine software. The chase of mant-ADP was initiated by adding a 0.5 mM ATP solution containing increasing amounts of AS-2 (up to 30 μM). The rates of mant-ADP release in the presence and absence of AS-2 were calculated by fitting the data to the following equation

$$y = A \exp(-k_1 t) + C$$

where k_1 represents the rate of mant-ADP release (in s^{-1}) as a function of time (t), A is the burst amplitude of mant-ADP release, and C is the endpoint of the reaction. The effects of AS-2 on mant-ADP release were determined by plotting the rates of release as a function of AS-2 concentration.

Inhibition of Basal and MT-Stimulated CENP-E and Eg5 ATPase Activities in the Presence of AS-2. All experiments were performed at room temperature. Steady-state analyses were carried out using the pyruvate kinase (PK)−lactate dehydrogenase (LDH) coupled assay in buffer A25 (*19*) supplemented or not with 300 mM NaCl (for basal and MT-stimulated ATPase activity measurements, respectively) and ATP (up to 1 mM). The final DMSO concentration in all cases was ∼2.4% in a constant volume of 100 μL. Kinetics were monitored using a 96-well Sunrise photometer (TECAN, Maennesdorf, Switzerland). Inhibitor modality under steady-state conditions was determined for CENP-E by measuring

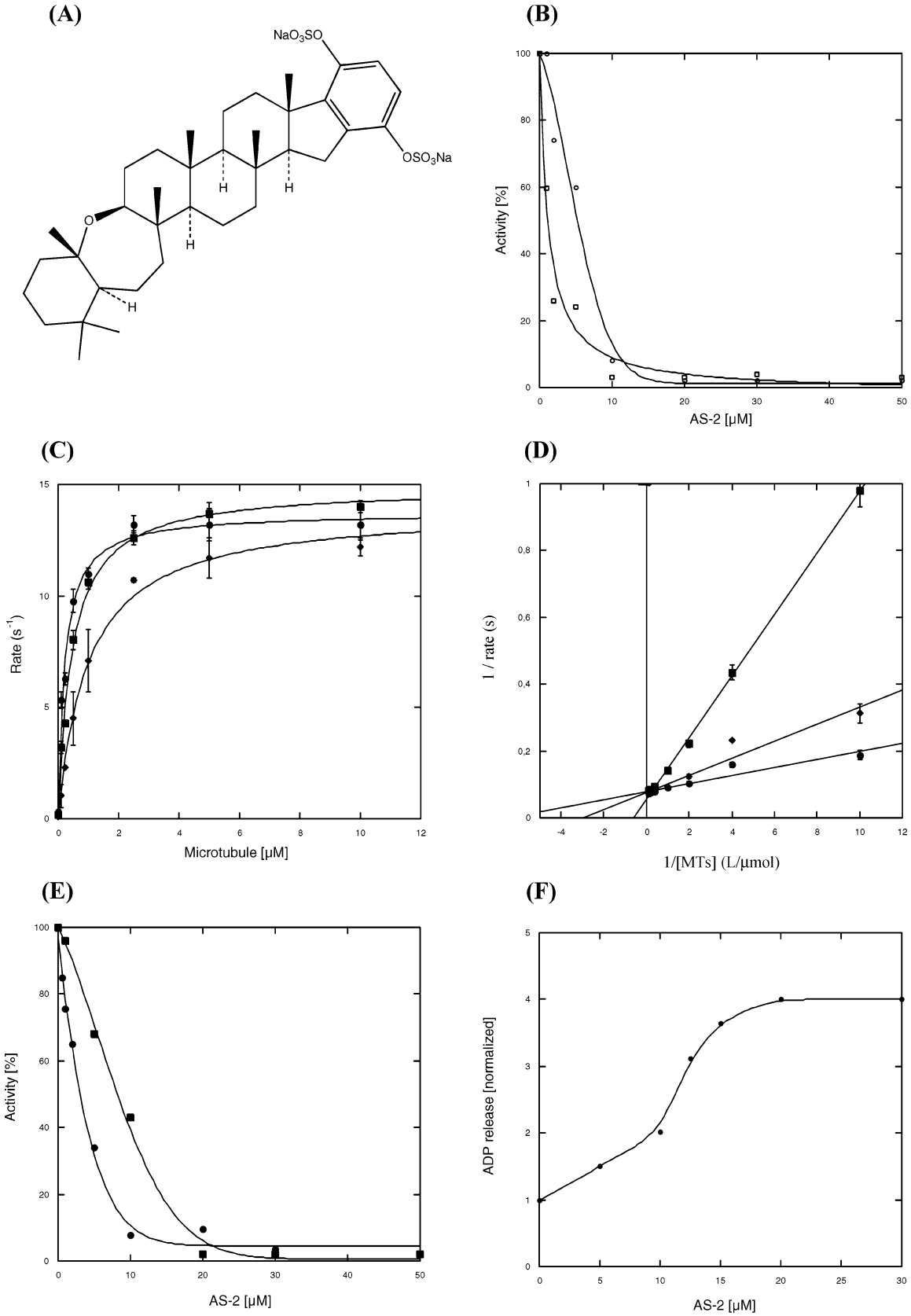

FIGURE 1: (A) Chemical structure of the marine natural product inhibitor adociasulfate-2 (AS-2). (B) AS-2 inhibits the MT-stimulated ATPase activity of human CENP-E (□) and Eg5 (○) with IC_{50} values of 1.3 μM and 5.3 μM, respectively. (C) Classical Michaelis−Menten representation of MT-stimulated CENP-E ATPase activity in the absence (●) and presence of either 0.5 μM (■) or 1.0 μM (◆) AS-2. (D) Double reciprocal plot of MT-stimulated CENP-E ATPase activity in the absence (●) and presence of 0.5 μM (◆) and 1.0 μM (■) AS-2. The presence of AS-2 modifies the $K_{0.5,MT}$ of CENP-E without affecting the ATP hydrolysis rate. AS-2 acts as a MT competitive inhibitor with an inhibitor constant K_i of 0.35 μM. (E) AS-2 inhibits the basal ATPase activity of Eg5 (●) and CENP-E (■) with IC_{50} values of 3.5 μM and 8.6 μM, respectively. (F) Effects of AS-2 on the ADP release rate of CENP-E in the absence of MTs. The presence of AS-2 accelerates the CENP-E ADP release rate. The magnitude of the burst appears to be dependent on the inhibitor concentration used, and the maximum burst was obtained with 20 μM AS-2.

the effect of AS-2 (up to 9 μM) on the initial velocity as a function of MT concentration at a fixed ATP concentration of 0.8 mM. The MT concentrations used in the assay were 0.1, 0.25, 0.5, 1, 2.5, 5, and 10 μM. IC_{50} values for AS-2 inhibition of basal and MT-stimulated CENP-E and Eg5 ATPase activities were determined by fitting the data to the following binding isotherm equation:

$$\frac{v_i}{v_0} = \frac{1}{1 + \frac{[I]}{IC_{50}}}$$

where v_i is the reaction velocity at different AS-2 concentrations [I], v_0 is the initial velocity in the absence of inhibitor, and IC_{50} is the inhibitor concentration required to achieve 50% inhibition. The amounts of CENP-E used were 25 nM and 0.8 μM in the presence or absence of MTs, respectively. For Eg5, the protein concentrations used were 1.8 μM and 38 nM in the absence and presence of MTs, respectively. Data were analyzed using Kaleidagraph 3.0 (Synergy Software). In a previous paper (*13*) the PK has been reported to be inhibited by AS-2 with an IC_{50} value greater than 136 μM. Therefore we tested if AS-2 inhibits the PK used in our experiments (type III from rabbit muscle, Sigma, ref No. P-9136). The enzyme-linked assay was carried out with 20 mM ADP in the absence of kinesin, either with or without 10 μM AS-2 (at this concentration, the inhibition of the MT-stimulated Eg5 and CENP-E ATPase activities is almost complete, see Figure 1B). No inhibitory (or stimulating) effect was observed. Consequently, the coupled test can be used with no risk that AS-2 interferes at this concentration with the PK or the LDH.

To confirm the inhibition of the CENP-E basal ATPase activity using the enzyme-linked assay, the effects of AS-2 on the basal CENP-E activity were also investigated using the CytoPhos phosphate assay, as described previously (*24*). CENP-E activity was measured in the presence of 5 μM and 10 μM AS-2.

Transmission Electron Microscopy. Solutions of AS-2 (50 μM) negatively stained with 1% (w/v) uranyl acetate as described previously (*25*) were examined using a Philips CM12 electron microscope equipped with a LaB6 filament operating at 120 kV. Several buffers supplemented or not with AS-2 were tested including 15 mM PIPES, pH 6.5 with and without 5 mM $MgCl_2$, and buffer A25, which was used for measuring Eg5 and CENP-E ATPase activity. Electron microscopy revealed no evidence of AS-2 polymerization or crystallization in any of the conditions tested.

Pepsin Digestion and Sequence Assignments. CENP-E and Eg5 digestions were performed for 2 min 15 s and 2 min, respectively, at 0 °C in 1 mM PIPES, pH 2.1 with a 2.9 μg/μL pepsin solution prepared in 0.1 M H_3PO_4, pH 1.6 [protease/substrate ratio: 1/1 (w/w)]. The peptide fragments generated after pepsin digestion were separated on a C18 Interchrom column (1 mm × 100 mm) by using a linear gradient from 5% to 60% CH_3CN/H_2O (9/1 v/v), 0.03% TFA (solvent B) over a run time of 60 min at a flow rate of 50 μL/min. Prior to the injection, the column was equilibrated with 95% solvent A (water with 0.03% TFA) and 5% solvent B for 20 min. Peptide assignments were performed by direct MS−MS analysis.

Hydrogen/Deuterium Exchange Experiments on Peptide Fragments. AS-2 (10 mM stock solution in DMSO) was diluted in 1 mM PIPES, pH 7.4. The complexes were formed at room temperature (1 min incubation time) using several protein/inhibitor ratios (mol/mol): 1/4, 1/8, and 1/12 for CENP-E; 1/4, 1/6, and 1/10 for Eg5. Both proteins were diluted 25-fold in deuterated buffer (1 mM PIPES, pD 6.8 or pD 7.4 for CENP-E and Eg5, respectively) in the presence and absence of AS-2. Deuteration was performed at 0 °C for 5 min in order to exchange all accessible amide hydrogens by deuterium. Assays were carried out in the presence of up to 1% DMSO. Isotopic back-exchange was quenched by the addition of 6 μL of precooled pepsin solution, pH 1.6. After digestion, deuterated pepsin cleaved fragments were rapidly concentrated and desalted on a C4 Peptide MacroTrap cartridge (Michrom) at a flow rate of 300 μL/min. Peptides were separated on a reverse phase C18 Interchrom column (1 mm × 100 mm) by using a linear gradient from 5% to 100% CH_3CN/H_2O (9/1 v/v), 0.03% TFA over a run time of 35 min at a flow rate of 50 μL/min. The elution of all peptides was complete after 17 min. To limit isotopic back-exchange during the analysis, the injector and columns were precooled in an ice bath and maintained at 0 °C. Adjustment for back-exchange was not performed since all experiments were conducted under similar conditions on the same day. The deuterated peptides were analyzed by ESI-MS.

ESI-MS and ESI-MS−MS Analysis. Sequence assignment and H/D exchange experiments were performed on a quadrupole ion trap mass spectrometer ESQUIRE 3000+ (Bruker Daltonics) equipped with an ion spray source. MS and MS−MS experiments were carried out with a capillary voltage set at 4000 V and an end plate offset voltage set at 500 V. The nebulizer gas (N_2) pressure was set at 10 psi and the dry gas flow (N_2) at 8 L/min at a temperature of 250 °C. Mass spectra were analyzed using DataAnalysis 3.0 and Biotools 2.1 software.

RESULTS

AS-2 is a natural compound isolated from the marine sponge *Adocia* sp. that has been shown to target members of the kinesin superfamily, namely *D. melanogaster* conventional kinesin (DmKHC) and *Xenopus laevis* CENP-E (*13*). This molecule is unique since it is the only kinesin inhibitor identified so far that has been shown to interfere with MT binding. In this study we characterized the effects of AS-2 on two human mitotic kinesins, CENP-E and Eg5. We used enzyme kinetics and H/D−MS to identify the secondary structural elements that are responsible for inhibitor binding. The H/D−MS experimental approach was the most appropriate as only very small amounts of AS-2 were needed for the analysis. We have already applied this method to identify the binding regions of several small inhibitors that target the motor domain of Eg5 (*9*−*10*).

Effects of AS-2 on the Basal and MT-Stimulated ATPase Activities of CENP-E and Eg5. The basal ATPase activity of monomeric CENP-E was 0.034 s^{-1} and is stimulated to 15.7 s^{-1} in the presence of MTs (Table 1). This activation is highly dependent on the salt concentration (data not shown). AS-2 inhibits the MT-stimulated ATPase activity of human CENP-E with a median inhibitory concentration (IC_{50}) of 1.3 μM (Figure 1B). To determine the type of

Table 1: Basal and MT-Stimulated ATPase Activities of CENP-E and Eg5 in the Absence and Presence of AS-2

	k_{cat} [s^{-1}]		$K_{0.5,MT}$ [μ**M**]		AS-2 inhibition [μ**M**]	
protein	−MTs	+MTs	−AS-2	+AS-2	basal ATPase activity	MT-stimulated ATPase activity
$CENP\text{-}E_{2-341}$	0.034	15.7[a]	0.21	0.46[b]/0.99[c]	8.6	1.3
$Eg5_{2-386}$	0.047[d]	14.1[d]	0.30[d]	nd[e]	3.5	5.3

[a] Maximum k_{cat}, which can vary depending on the MT preparation and polymerization or the presence of DMSO. [b] In the presence of 0.5 μM AS-2. [c] In the presence of 1.0 μM AS-2. [d] Values taken from ref *20*. [e] Not determined.

inhibition by AS-2, we measured the rate of ATP hydrolysis in the presence or absence of inhibitor and increasing amounts of MTs (Figure 1C). The Lineweaver−Burk representation shows that AS-2 acts as a MT-competitive inhibitor with an inhibition constant (K_i) of 0.35 μM (Figure 1D). The catalytic constant (k_{cat}) remains unaffected whereas a 2- to 5-fold increase is observed for $K_{0.5,MT}$ with values of 0.21 μM, 0.46 μM, and 0.99 μM in the absence and presence of 0.5 μM and 1.0 μM AS-2, respectively (Table 1). We further tested AS-2 on the motor domain of the mitotic Eg5. As observed for CENP-E, AS-2 inhibits the MT-stimulated Eg5 ATPase activity with an IC_{50} value of 5.3 μM (Figure 1B). We also found that AS-2 was able to inhibit the basal ATPase activity of both CENP-E and Eg5 with an IC_{50} of 8.6 and 3.5 μM, respectively, using the enzyme-linked assay (Figure 1E). For *D. melanogaster* conventional kinesin (*13*), a stimulation of the basal ATP activity was reported in the presence of AS-2. To exclude the possibility that the observed inhibition of basal CENP-E ATPase activity results from inhibition of one of the test compounds of the enzyme-linked test (PK or LDH), but not CENP-E, we measured the inhibition by AS-2 at 5 and 10 μM using the CytoPhos phosphate assay, which is based on the production of inorganic phosphate without adding additional enzymes (*26*). Again, we observed an inhibition of the basal CENP-E ATPase. On the other hand, an acceleration of the ADP release rate (as shown for conventional kinesin) is observed when CENP-E is incubated with increasing amounts of AS-2 (Figure 1F). This result indicates that the inhibitor stimulates ADP release when bound to the motor domain thus "mimicking" the activity of MTs. The binding of MTs to kinesin is known to stimulate the basal ATPase activity by ~1000-fold, primarily by accelerating the ADP release rate (*27*, *28*). However, the observed acceleration of the CENP-E/ADP release rate is correlated with an inhibition of the basal ATPase activity (Figure 1E). It thus seems possible that the AS-2 binding on the CENP-E/MT interacting region locks the motor domain in a conformation suitable for ADP release but not for ATP binding and/or hydrolysis. To further test the specificity of AS-2, we investigated the inhibition of the MT-stimulated ATPase activity of members of different kinesin families and found that they are all inhibited by AS-2 (data not shown). These results show that AS-2 targets many members of the kinesin superfamily, including *D. melanogaster* KHC and *X. laevis* CENP-E (*13*) and *Homo sapiens* MKLP1, RabK6, MPP1, KIFC1, KIFC3, CENP-E, and Eg5.

Interaction of AS-2 with CENP-E. The regions of CENP-E responsible for the attachment of MTs were investigated by H/D−MS using AS-2 as a molecular probe. The CENP-E peptide map is presented in Figure 2. Among the 133 proteolytic fragments generated and assigned by LC−ESI-MS−MS (sequence coverage of 96%), 76 peptide fragments were found after 5 min deuteration allowing 94% of the motor domain to be covered. The 2% loss in sequence coverage affects region L9-β6 and corresponds to peptide fragment Asp197−Phe206. This fragment contains the switch I motif (NQRSSRSH) of the nucleotide-binding pocket (*21*). The effects of AS-2 binding on the motor domain were monitored after 5 min deuteration. Binding of AS-2 decreases the solvent accessibility of 13 peptide fragments which delimit 3 regions of the motor domain: Met132−Leu167 (β4-L7-β5-L8-β5a-L8-β5b), Arg241−Phe263 (L11-α4), and Ile281−Leu288 (L12-α5). Deuterium exchange results for four selected peptide fragments, Met132−Leu142 (L7-β5), Val234−Glu240 (β7-onset of L11), Val234−Asn257 (β7-α−L11), and Ile281−Leu288 (L12-α5), are reported in Figure 3A. No reduction in the solvent accessibility is observed in peptide fragment Val234−Glu240. Hence, the decrease of deuterium incorporation observed in fragment Val234−Asn257 only takes place in the C-terminal part of the peptide (loop 11). The other peptide fragments show no difference in the extent of deuterium incorporation in the presence of the inhibitor. Interestingly, the three identified regions are located on the side of the motor domain opposite to the monastrol and STLC binding regions on Eg5 (Figure 4A). The observed solvent accessibility reduction in these regions can be due to a masking effect, to allosteric conformational changes induced upon ligand binding, or to both. We thus compared the "putative" MT-binding interface inferred by H/D−MS with the recent results obtained by docking CENP-E and tubulin structures into 3D image reconstructions obtained by electron cryomicroscopy (cryo-EM) of the CENP-E/MT complex (*29*). Most of the observed solvent accessibility modifications in the presence of AS-2 appear related to a masking effect, except for β4 and L7. These secondary structural elements were not identified by cryo-EM, and their monitored exchange rates probably correspond to conformational changes induced upon AS-2 binding. Loop L11, helix α4, loop L12, helix α5, loop L8, and strand β5 seem thus to correspond to the main MT-binding elements of CENP-E (Figure 4A). These regions were also identified as part of the MT interface of Ncd (*17*), KIF1A (*30*), and conventional kinesin (*16*) suggesting that the MT contact areas are well conserved among kinesin motors.

Interaction of AS-2 with Eg5. Given that (1) AS-2 is a nonspecific kinesin inhibitor and (2) the kinesin-MT interface seems to be well conserved, we also investigated the MT-binding regions of human Eg5. Due to the limited amount of AS-2 available, it was not possible to determine the type of Eg5 inhibition by AS-2. However, the inhibitor affects both basal and MT-stimulated Eg5 ATPase activities (Figures 1B and 1E). The Eg5 peptide map used for H/D−MS experiments has been described previously (*9*) (see Support-

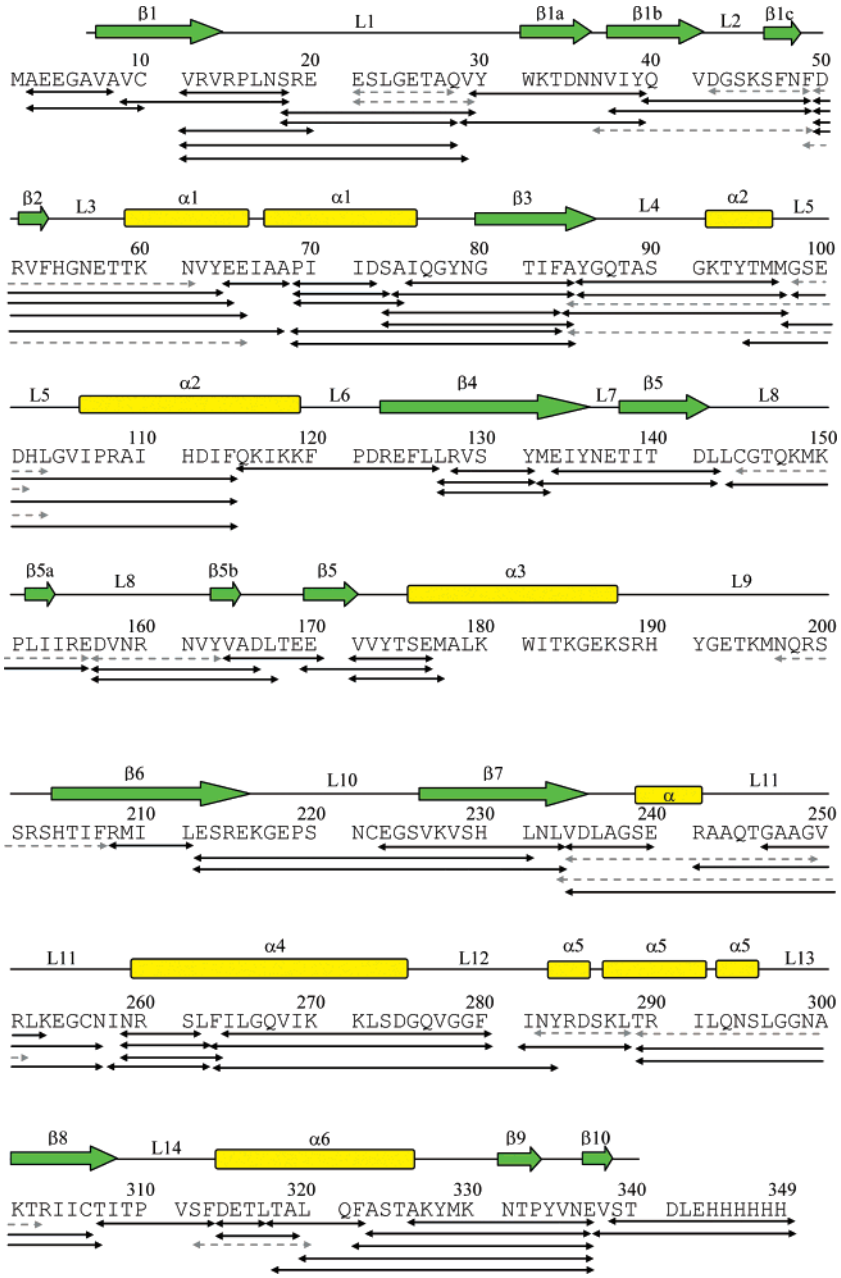

FIGURE 2: Amino acid sequence of the CENP-E motor domain showing the 93 pepsin-cleaved fragments recovered after HPLC separation on ice. Secondary structural elements determined by X-ray crystallography *(21)* are shown above the sequence. Arrows below the sequence indicate the position of the proteolytic fragments assigned by LC−ESI-MS−MS. Peptides which were not recovered after 5 min deuteration on ice are denoted with dashed arrows.

ing Information Figure S1). We found that AS-2 binding to Eg5 increased the deuterium uptake of similar regions identified for CENP-E, except for loop L11. Results for peptides Phe169−Asp177 (β5−L8) and Leu293−Leu302 (α4) are reported in Figure 3B. The other Eg5 peptide fragments show no difference in the extent of deuterium incorporation indicating that no other part on the motor domain was affected by the presence of the inhibitor. The two identified regions [consisting of Leu161−Arg189 (β4-L7-β5-L8-β5a) and Leu293−Leu316 (α4-L12-α5)] are also located on the side of the motor domain containing the main secondary structural elements that are involved in the kinesin−MT interface (*16*) (Figure 4B). To our surprise, AS-2 produces the opposite effect on Eg5 as compared to CENP-E. Formation of the Eg5/AS-2 complex leads to greater solvent accessibility in all modified peptides, with fragment Leu293−Leu302 exhibiting the most significant increase in deuterium uptake (Figure 3B). This peptide is composed of the C-terminal end of helix α4 and is poorly deuterated, because amide hydrogens located in helices participate in intramolecular hydrogen bonding and are thus "protected" from deuteration. In the presence of AS-2, most of the amide hydrogens become accessible, suggesting a strong structural modification.

DISCUSSION

Natural compounds extracted from marine animals, algae, fungi, or bacteria represent a rich source of bioactive compounds with a broad spectrum of biological activities, including antifungal, antibacterial, and antiviral activities (*31*). Some of these compounds are in clinical phase II or III trials as candidates for the development of small molecule

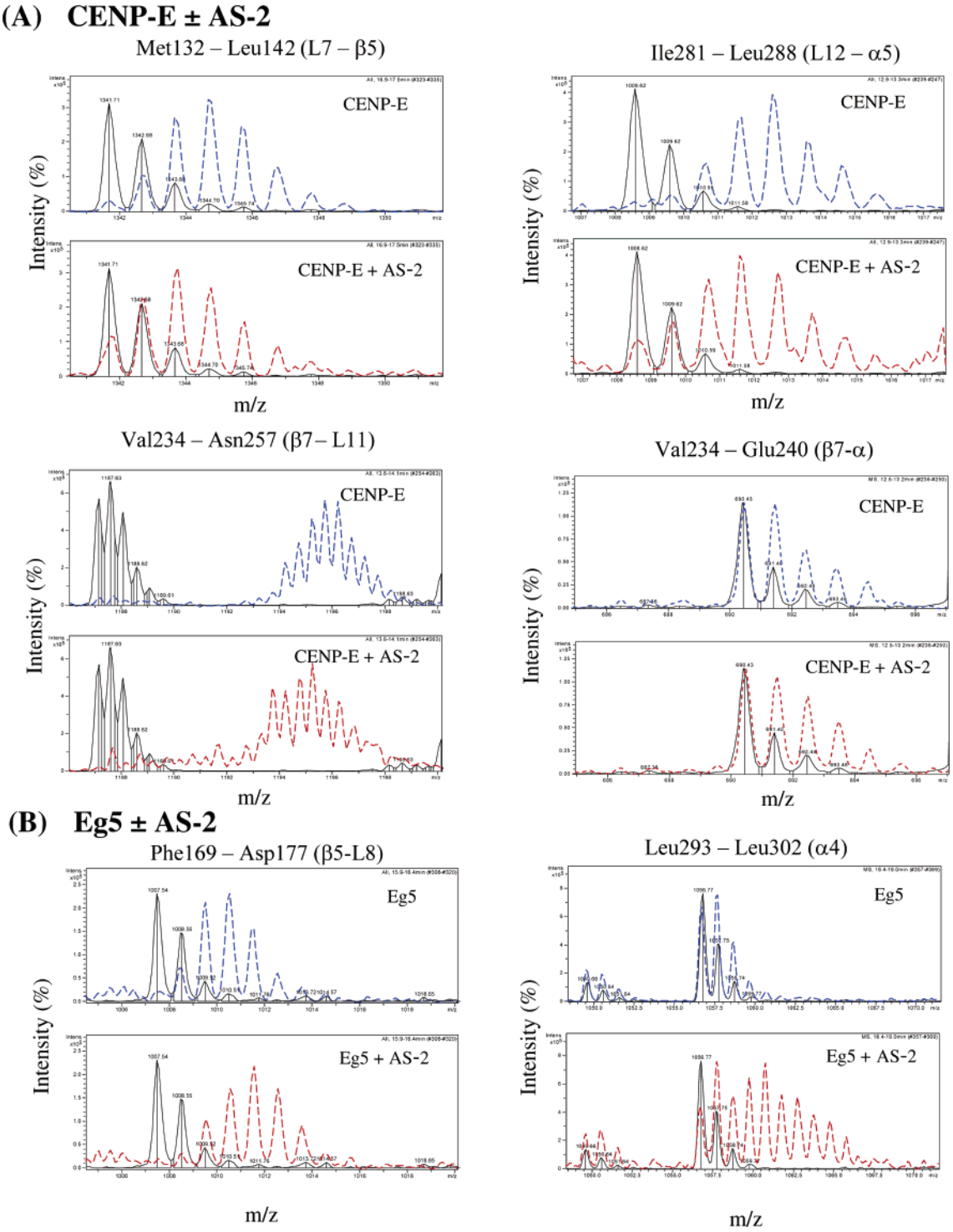

FIGURE 3: Effects of AS-2 binding on the deuterium incorporation rate. (A) CENP-E peptide fragments Met132−Leu142, Ile281−Leu288, Val234−Asn257, and Val234−Glu240. (B) Eg5 peptide fragments Phe169−Asp177 and Leu293−Leu302. Binding of AS-2 to the Eg5 motor domain increases the extent of deuterium incorporation, whereas the solvent accessibility is reduced in the CENP-E motor domain. Each mass spectrum compares nondeuterated peptide fragments (solid line) with peptide fragment after 5 min deuteration without (blue dashed line) and with adociasulfate-2 (red dashed line).

pharmaceuticals (*32*). Another important application of natural compounds derived from marine organisms concerns their use as molecular probes to study protein function (chemical genetics) or to elucidate the mechanism of action of enzymes. Adociasulfates represent a new group of bioactive marine natural products isolated from different sponge species. Ten different adociasulfate compounds have been identified and isolated (*13*, *33*−*36*), but until now only adociasulfate-1 was synthesized from commercially available compounds by enantioselective synthesis (*37*). As a consequence only very small amounts of AS-2 were available for this study. Mass spectrometry associated with H/D exchange experiments was therefore the most appropriate method to characterize the effects of AS-2 on kinesin motor domains as only minuscule quantities of inhibitor were required for the analysis. With this approach we were able to monitor the effects of AS-2 binding on the structure of two human mitotic kinesins, CENP-E and Eg5.

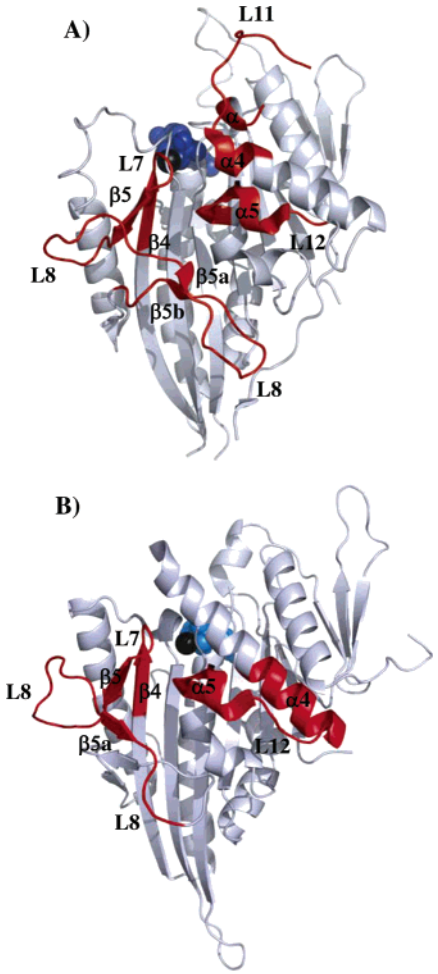

FIGURE 4: Ribbon representations of CENP-E and Eg5 motor domains showing the secondary structure elements modified in the presence of AS-2. MgADP is shown as a space-filling model (blue). (A) Incubation of CENP-E in the presence of 8-fold molar excess AS-2 reduces the solvent accessibility of three regions: Glu133−Leu167 (*β*4-L7-*β*5-L8-*β*5b), Ile281−Leu288 (L12-α5), and Arg241−Phe262 (L11-α4). (B) Binding of AS-2 increases the deuterium incorporation rate of two regions within the Eg5 motor domain: Leu161−Arg189 (*β*4-L7-*β*5-L8-*β*5a) and Leu293−Leu316 (α4-L12-α5).

CENP-E and Eg5 Both Share a Common MT-Binding Interface. We show here that the MT-competitive inhibitor AS-2 represents an excellent molecular probe to infer the interface between kinesins and MTs by H/D−MS. The binding of AS-2 affects the deuterium incorporation rate of similar regions on CENP-E and Eg5 motor domains, mainly loops L8 and L11 and the switch II cluster (α4-L12-α5), suggesting that both kinesins use the same secondary structural elements to interact with MTs (Figure 4). However, the effects of AS-2 binding are different for both motor domains, suggesting that AS-2 does not act identically on both proteins to achieve the same inhibitory effect. Formation of the CENP-E/AS-2 complex leads to a small decrease of the deuterium incorporation rate whereas an increase of solvent accessibility is observed for Eg5. The observed increase of deuterium uptake is surprising since we expected to see a masking effect on Eg5. This indicates that important structural changes occur within the AS-2 binding interface leading to the exposure of more amide hydrogen to the deuterated buffer than those protected upon AS-2 binding. The most significant deuterium uptake observed in Eg5 occurs in the C-terminal end of helix α4 (Figures 3B and 4B). Such a structural modification on helix α4 has also been reported for the KIF1A kinesin motor domain (*18*). The determination of the KIF1A crystal structure in different nucleotide states revealed significant conformational changes in the switch II region (loop L11, helix α4, and loop L12). During phosphate release (ADP-Pi state), both loop L11 and L12 are shortened allowing the elongation of α4 from both ends. After phosphate release (ADP state), the end of α4 is shortened and L12 recovers its flexible conformation. These modifications allow KIF1A to modulate its MT affinity. In our experiments, the Eg5 motor domain was in an ADP state, suggesting that L12 was already in a flexible conformation. Consequently, the observed structural modification of α4 is not related to the nucleotide state of the motor domain but directly to AS-2 binding. Finally, it is interesting to note that most of these regions were identified as part of the MT-binding interface of other kinesins, such as the conventional kinesin (L7/L8, L11, and L12/α5) (*16*), Ncd (L11, L12 and α4, L8, L2 and α6) (*17*), and KIF1A (L8, α6/L12, and the switch II cluster) (*18*, *30*).

Limits of the H/D−MS Approach. To reduce the complexity of the system we used the MT-competitive inhibitor AS-2 and not MTs to locate the binding regions implicated in the interaction with MTs. A total of 133 proteolytic peptides where identified for CENP-E, and the presence of MTs would have considerably increased the number of peptides generated, probably to several hundreds. The protein sequences of α- and *β*-tubulin of the heterodimer are very similar to each other, making the analysis with the H/D−MS approach, in particular the unambiguous identification and assignment of peptides, even more complicated. We have been able to identify the surface of kinesins that is implicated in the interaction with MTs; however, we cannot distinguish between the "up" and "down" orientation when CENP-E is docked onto a MT, which requires high-resolution cryo-EM of the complex.

The Structure of AS-2 in Solution. In a recent paper the structure of AS-2 responsible for the inhibition of kinesin was reported to exist as rodlike aggregates (in the presence of magnesium ions) with the sulfate groups probably exposed to the aqueous environment, thus mimicking MTs (*25*). However, no AS-2 aggregates or filaments were observed by TEM in any buffer conditions used in our experiments (data not shown). It is likely that the monodisperse form of AS-2 is thus responsible for the observed inhibitory effect on both CENP-E and Eg5. Due to the lack of sufficient inhibitor, an exhaustive analysis was impossible. The existence of rodlike aggregates would be in accord with our results since the surface of the regions identified is too large to be explained by a simple masking effect by AS-2. Assuming that AS-2 is a classical 1:1 inhibitor leads to the following possibilities. An explanation for the large area involved is that a number of AS-2 molecules are bound; this would indicate a decrease in the solvent accessibility in each case. However, in one case the solvent accessibility is decreased (CENP-E) and is increased in the other (Eg5). All these observations can therefore be explained if we suppose that binding of the AS-2 molecule induces an allosteric change in the motor domain, which interferes with MT binding.

AS-2 as a Tool To Study Kinesins. Monastrol, one of the first kinesin inhibitors identified, has been a valuable tool for the elucidation of mechanistic details of mitotic Eg5. For example, the crystal structure of the ADP-Eg5-monastrol ternary complex (*38*) revealed large conformational rearrangements, when compared to the native structure (*39*). Monastrol binds in a pocket formed by helix α2/loop L5 and helix α3 and inhibits ADP release (*20*, *40*) but not ATP binding (*41*). A structural comparison with KIF1A reveals that the α4−α5 cluster and the neck-linker (involved in MT binding) in the ternary complex can be superposed on the KIF1A−AMPPCP complex, but not with bound ADP, indicating that the ADP−Eg5−monastrol ternary complex is in the "locked" conformation (presumably ATP-like), whereas the native Eg5 structure is in the "unlocked" conformation (ADP state). In contrast to monastrol, AS-2 inhibits CENP-E and Eg5, but binds to the opposite region of known Eg5 inhibitors, the putative MT-binding site, and stimulates ADP release in the case of CENP-E and *D. melanogaster* KHC. Since adociasulfates act with a different mechanism than monastrol, they might also be valuable tools to study Eg5 mechanism and function, and their use might lead to new structural conformations and additional mechanistic insights into Eg5 function, that are not accessible by monastrol-related compounds.

ACKNOWLEDGMENT

The partial cDNA for CENP-E was from Dr. Tim Yen, Fox Chase Cancer Center, Philadelphia. We thank Drs. Thomas E. Wales (The Barnett Institute, Northeastern University, Boston) and Richard H. Wade (IBS, Grenoble) for helpful discussions. We are grateful to Eric Forest (LSMP, IBS) for supporting the project.

SUPPORTING INFORMATION AVAILABLE

Peptide map of the Eg5 motor domain. This material is available free of charge via the Internet at http://pubs.acs.org.

REFERENCES

1. Miki, H., Okada, Y., and Hirokawa, N. (2005) Analysis of the kinesin superfamily: insights into structure and function, *Trends Cell Biol. 15*, 467−476.
2. Smith, D. L., Deng, Y., and Zhang, Z. (1997) Probing the noncovalent structure of proteins by amide hydrogen exchange and mass spectrometry, *J. Mass Spectrom. 32*, 135−146.
3. Engen, J. R., and Smith, D. L. (2000) Investigating the higher order structure of proteins. Hydrogen exchange, proteolytic fragmentation, and mass spectrometry, *Methods Mol. Biol. 146*, 95−112.
4. Maier, C. S., and Deinzer, M. L. (2005) Protein conformations, interactions, and H/D exchange, *Methods Enzymol. 402*, 312−360.
5. Anand, G. S., Hughes, C. A., Jones, J. M., Taylor, S. S., and Komives, E. A. (2002) Amide H/2H exchange reveals communication between the cAMP and catalytic subunit-binding sites in the R(I)alpha subunit of protein kinase A, *J. Mol. Biol. 323*, 377−386.
6. Mandell, J. G., Falick, A. M., and Komives, E. A. (1998) Identification of protein-protein interfaces by decreased amide proton solvent accessibility, *Proc. Natl. Acad. Sci. U.S.A. 95*, 14705−14710.
7. Akashi, S., and Takio, K. (2000) Characterization of the interface structure of enzyme-inhibitor complex by using hydrogen-deuterium exchange and electrospray ionization Fourier transform ion cyclotron resonance mass spectrometry, *Protein Sci. 9*, 2497−2505.
8. Garcia, R. A., Pantazatos, D., and Villarreal, F. J. (2004) Hydrogen/deuterium exchange mass spectrometry for investigating protein-ligand interactions, *Assay Drug Dev. Technol. 2*, 81−91.
9. Brier, S., Lemaire, D., DeBonis, S., Forest, E., and Kozielski, F. (2004) Identification of the protein binding region of S-trityl-L-cysteine a new potent inhibitor of the mitotic kinesin Eg5, *Biochemistry 43*, 13072−13082.
10. Brier, S., Lemaire, D., DeBonis, S., Kozielski, F., and Forest, E. (2006) Use of hydrogen/deuterium exchange mass spectrometry and mutagenesis as a tool to identify the binding region of inhibitors targeting the human mitotic kinesin Eg5, *Rapid Commun. Mass Spectrom. 20*, 456−462.
11. Zhang, Z., and Smith, D. L. (1993) Determination of amide hydrogen exchange by mass spectrometry: a new tool for protein structure elucidation, *Protein Sci. 2*, 522−531.
12. Cravello, L., Lascoux, D., and Forest, E. (2003) Use of different proteases working in acidic conditions to improve sequence coverage and resolution in hydrogen/deuterium exchange of large proteins, *Rapid Commun. Mass Spectrom. 17*, 2387−2393.
13. Sakowicz, R., Berdelis, M. S., Ray, K., Blackburn, C. L., Hopmann, C., Faulkner, D. J., and Goldstein, L. S. (1998) A marine natural product inhibitor of kinesin motors, *Science 280*, 292−295.
14. Blangy, A., Lane, H. A., d'Herin, P., Harper, M., Kress, M., and Nigg, E. A. (1995) Phosphorylation by p34cdc2 regulates spindle association of human Eg5, a kinesin-related motor essential for bipolar spindle formation in vivo, *Cell 83*, 1159−1169.
15. Maney, T., Ginkel, L. M., Hunter, A. W., and Wordeman, L. (2000) The kinetochore of higher eucaryotes: a molecular view, *Int. Rev. Cytol. 194*, 67−131.
16. Woehlke, G., Ruby, A. K., Hart, C. L., Ly, B., Hom-Booher, N., and Vale, R. D. (1997) Microtubule interaction site of the kinesin motor, *Cell 90*, 207−216.
17. Sosa, H., Prabha Dias, D., Hoenger, A., Whittaker, M., Wilson-Kubalek, E., Sablin, E., Fletterick, J. R., Vale, R. D., and Milligan, R. A. (1997) A model for the microtubule-ncd motor protein complex obtained by cryo-electron microscopy and image analysis, *Cell 90*, 217−224.
18. Nitta, R., Kikkawa, M., Okada, Y., and Hirokawa, N. (2004) KIF1A alternately uses two loops to bind microtubules, *Science 305*, 678−683.
19. Hackney, D. D., and Jiang, W. (2001) Assays for kinesin microtubule-stimulated ATPase activity, *Methods Mol. Biol. 164*, 65−71.
20. DeBonis, S., Simorre, J. P., Crevel, I., Lebeau, L., Skoufias, D. A., Blangy, A., Ebel, C., Gans, P., Cross, R., Hackney, D. D., et al. (2003) Interaction of the mitotic inhibitor monastrol with human kinesin Eg5, *Biochemistry 42*, 338−349.
21. Garcia-Saez, I., Yen, T., Wade, R. H., and Kozielski, F. (2004) Crystal structure of the motor domain of the human kinetochore-associated protein CENP-E, *J. Mol. Biol. 340*, 1107−1116.
22. Asnes, C. F., and Wilson, L. (1979) Isolation of bovine brain microtubule protein without glycerol: polymerization kinetics change during purification cycles, *Anal. Biochem. 98*, 64−73.
23. DeBonis, S., Skoufias, D. A., Lebeau, L., Lopez, R., Robin, G., Margolis, R. L., Wade, R. H., and Kozielski, F. (2004) In vitro screening for inhibitors of the human mitotic kinesin Eg5 with antimitotic and antitumor activities, *Mol. Cancer Ther. 3*, 1079−1090.
24. Brier, S., Lemaire, D., DeBonis, S., Forest, E., and Kozielski, F. (2006) Molecular dissection of the inhibitor binding pocket of mitotic kinesin Eg5 reveals mutants that confer resistance to antimitotic agents, *J. Mol. Biol. 360*, 360−376.
25. Reddie, K. G., Roberts, D. R., and Dore, T. M. (2006) Inhibition of kinesin motor proteins by adocialsulfate-2, *J. Med. Chem. 49*, 4857−4860.
26. Funk, C. J., Davis, A. S., Hopkins, J. A., and Middleton, K. M. (2004) Development of high-throughput screens for discovery of kinesin adenosine triphosphate modulators, *Anal. Biochem. 329*, 68−76.
27. Hackney, D. D. (1994) Evidence for alternating head catalysis by kinesin during microtubule-stimulated ATP hydrolysis, *Proc. Natl. Acad. Sci. U.S.A. 91*, 6865−6869.
28. Gilbert, S. P., Webb, M. R., Brune, M., and Johnson, K. A. (1995) Pathway of processive ATP hydrolysis by kinesin, *Nature 373*, 671−676.
29. Neumann, E., Garcia-Saez, I., DeBonis, S., Wade, R. H., Kozielski, F., and Conway, J. F. (2006) Human kinetochore-associated

kinesin CENP-E visualized at 17 Å bound to microtubules, *J. Mol. Biol. 362*, 203−211.
30. Kikkawa, M., Sablin, E. P., Okada, Y., Yajima, H., Fletterick, R. J., and Hirokawa, N. (2001) Switch-based mechanism of kinesin motors, *Nature 411*, 439−445.
31. Blunt, J. W., Copp, B. R., Munro, M. H., Northcote, P. T., Prinsep, and M. R. (2005) Marine natural products, *Nat. Prod. Rep. 22*, 15−61.
32. Newman, D. J., and Cragg, G. M. (2004) Marine natural products and related compounds in clinical and advanced preclinical trials, *J. Nat. Prod. 67*, 1216−1238.
33. Blackburn, C. L., Hopmann, C., Sakowicz, R., Berdelis, M. S., Goldstein, L. S., and Faulkner, D. J. (1999) Adociasulfates 1-6, inhibitors of kinesin motor proteins from the sponge *Haliclona* (aka *Adocia*) sp, *J. Org. Chem. 64*, 5565−5570.
34. Kalaitzis, J. A., de Almeida Leone, P., Harris, L., Butler, M. S., Ngo, A., Hooper, J. N., and Quinn, R. J. (1999) Adociasulfates 1, 7, and 8: new bioactive hexaprenoid hydroquinones from the marine sponge Adocia sp., *J. Org. Chem. 64*, 5571−5574.
35. Kalaitzis, J. A., and Quinn, R. J. (1999). Adociasulfate-9, a new hexaprenoid hydroquinone from the great barrier reef sponge *Adocia* sp., *J. Nat. Prod. 62*, 1682−1684.
36. Blackburn, C. L., and Faulkner, D. J., (2000) Adociasulfate 10, a new merohexaprenoid sulfate from the sponge *Haliclona* (aka *Adocia*) sp., *Tetrahedron 56*, 8429−8432.
37. Bogenstätter, M., Limberg, M. A., Overman, L. E., and Tomasi, A. L. (1999) Enantioselective total synthesis of the kinesin motor protein inhibitor adociasulfate 1, *J. Am. Chem. Soc. 121*, 12206−12207.
38. Yan, Y., Sardana, V., Xu, B., Homnick, C., Halczenko, W., Buser, C. A., Schaber, M., Hartman, G. D., Huber, H. E., and Kuo, L. C. (2004) Inhibition of a mitotic motor protein: where, how, and conformational consequences, *J. Mol. Biol. 335*, 547−554.
39. Turner, J., Anderson, R., Guo, J., Beraud, C., Fletterick, R., and Sakowicz, R. (2001) Crystal structure of the mitotic spindle kinesin Eg5 reveals a novel conformation of the neck-linker, *J. Biol. Chem. 276*, 25496−25502.
40. Maliga, Z., Kapoor, T. M., and Mitchison, T. J. (2002) Evidence that monastrol is an allosteric inhibitor of the mitotic kinesin Eg5, *Chem. Biol. 9*, 989−996.
41. Cochran, J. C., Gatial J. E., 3rd, Kapoor, T. M., and Gilbert, S. P. (2004) Monastrol inhibition of the mitotic kinesin Eg5, *J. Biol. Chem. 280*, 12658−12667.

BI061395N